# The 2.46 Å Resolution Structure of the Pancreatic Lipase−Colipase Complex Inhibited by a C11 Alkyl Phosphonate[†,‡]

Marie-Pierre Egloff,[§] Frank Marguet,[∥] Gérard Buono,[∥] Robert Verger,[⊥] Christian Cambillau,*[,§] and Herman van Tilbeurgh[§,#]

*Laboratoire de Cristallisation et Cristallographie des Macromolécules Biologiques, URA 1296-CNRS, Faculté de Médecine Nord, 13916 Marseille Cedex 20, France, Réactivité et Catalyse, ENSSPICAM URA CNRS 1410, Avenue Escadrille Normandie-Niemen, 13397 Marseille Cedex 13, France, and Laboratoire de Lipolyse Enzymatique, URA 9025 du GDR 1000-CNRS, 31 Chemin Joseph Aiguier, 13402 Marseille Cedex 20, France*

*Received July 25, 1994; Revised Manuscript Received December 7, 1994*[⊗]

ABSTRACT: Pancreatic lipase belongs to the serine esterase family and can therefore be inhibited by classical serine reagents such as diisopropyl fluoride or E600. In an attempt to further characterize the active site and catalytic mechanism, we synthesized a C11 alkyl phosphonate compound. This compound is an effective inhibitor of pancreatic lipase. The crystal structure of the pancreatic lipase−colipase complex inhibited by this compound was determined at a resolution of 2.46 Å and refined to a final *R*-factor of 18.3%. As was observed in the case of the structure of the ternary pancreatic lipase−colipase−phospholipid complex, the binding of the ligand induces rearrangements of two surface loops in comparison with the closed structure of the enzyme (van Tilbeurgh et al., 1993b). The inhibitor, which could be clearly observed in the active site, was covalently bound to the active site serine Ser152. A racemic mixture of the inhibitor was used in the crystallization, and there exists evidence that both enantiomers are bound at the active site. The C11 alkyl chain of the first enantiomer fits into a hydrophobic groove and is thought to thus mimic the interaction between the leaving fatty acid of a triglyceride substrate and the protein. The alkyl chain of the second enantiomer also has an elongated conformation and interacts with hydrophobic patches on the surface of the open amphipathic lid. This may indicate the location of a second alkyl chain of a triglyceride substrate. Some of the detergent molecules, needed for the crystallization, were also observed in the crystal. Some of them were located at the entrance of the active site, bound to the hydrophobic part of the lid. On the basis of this crystallographic study, a hypothesis about the binding mode of real substrates and the organization of the active site is proposed.

All the triglyceride lipases, the three-dimensional structures of which have been determined so far, belong to the serine esterase class (Brady et al., 1990; Winkler et al., 1990; Schrag et al., 1991; Martinez et al., 1992; Noble et al., 1993). The active serine is part of a catalytic triad, which is similar to that observed in the case of serine proteases: the triads of lipases and proteases are actually mirror images of each other (Winkler et al., 1990; Brady et al., 1990). In lipases, the active serine belongs to a characteristic nucleophile "elbow" and invariably has a very unfavorable main-chain conformation (Derewenda & Derewenda, 1991; Ollis et al., 1992). Furthermore, the catalytic serine present in lipases is prevented from reaching the solvent by one or more surface loops that have to be rearranged to give free entrance to the substrate (Derewenda et al., 1992; van Tilbeurgh et al., 1993b; Grochulski et al., 1993). Although the solvent accessibility of the catalytic serine is different in proteases and lipases, a classical protease inhibitor such as E600 is capable of inactivating lipases. Covalent adducts of *Rhizomucor miehei* lipase, *Candida rugosa* lipase, and cutinase with organophosphate or organophosphonate inhibitors have been structurally characterized (Derewenda et al., 1992; Brzozowski et al., 1991; Grochulski et al., 1994; Martinez et al., 1993). On the basis of these structures, the oxyanion hole has been identified: an electrophilic environment is involved in stabilizing the negative charge during catalysis (Kraut, 1977). The recently determined three-dimensional structures of the *Candida rugosa* lipase inhibited by the different enantiomers of a phosphonate inhibitor have provided the structural basis of the chiral preferences of lipases (Cygler et al., 1994).

These studies using small organophosphate inhibitors have yielded some valuable ideas about the catalytic mechanism of lipases. The three-dimensional structures have revealed how the active site loops rearrange to give free access to the catalytic triad. These small inhibitors bear little resemblance, however, to a natural triglyceride substrate. Attempts to increase the hydrophobicity of these inhibitors have been made, and the structure of a C6-phosphonate inhibitor with *R. miehei* was determined (Brzozowski et al., 1991). In order to mimic a natural substrate more closely, we synthesized

[†] This work was supported by the EC BRIDGE-T "Lipase" project (No. BIOT CT91-023), the CNRS-IMABIO programme, and the PACA region.

[‡] Coordinates have been deposited with the Brookhaven Protein Data Bank under the filename 1LPB.

* Corresponding author (telephone, 91 69 89 09/08; Fax, 91 69 89 13; E-mail, cambilau@lccmb.cnrs-mrs.fr).

[§] Laboratoire de Cristallisation et Cristallographie des Macromolécules Biologiques.

[∥] Réactivité et Catalyse.

[⊥] Laboratoire de Lipolyse Enzymatique.

[#] Permanent address: Centre de Biochimie Structurale, CNRS-UMR C9955/INSERM-U414, Université de Montpellier I, Faculté de Pharmacie, 15 Avenue Charles Flahault, F 34060 Montpellier Cedex 1, France.

[⊗] Abstract published in *Advance ACS Abstracts,* February 1, 1995.

0006-2960/95/0434-2751$09.00/0 

phosphonate inhibitors with long alkyl chains which are powerful lipase inhibitors (Cudrey et al., 1993; Marguet et al., 1994).

Some information about the spectacular conformational changes occurring at the active site of pancreatic lipase has been deduced from the recently determined structure of a ternary lipase−colipase−phospholipid complex at 3.0 Å resolution (van Tilbeurgh et al., 1993). We have now obtained crystals of the pancreatic lipase−colipase complex covalently modified by a phosphonate inhibitor bearing a C11 alkyl chain (see further). These crystals diffract at a higher resolution (2.46 Å) than those obtained in the presence of phospholipid (3.03 Å) (van Tilbeurgh et al., 1993). This has made it possible to describe in greater detail the overall structure of the complex, as well as the bound inhibitor and detergent molecules, i.e., octyl β-glucoside. On the basis of these structural data, some suggestions are made as to the functional organization of the active site and the catalytic mechanism involved.

## MATERIALS AND METHODS

*Compounds and Crystallization.* The purification of human pancreatic lipase (DeCaro et al., 1977) and that of porcine-activated colipase (Canioni et al., 1979) and the synthesis of the *O*-(2 methoxyethyl) *O*-(*p*-nitrophenyl) *n*-undecylphosphonate (C11P) were carried out as previously described (Marguet et al., 1994). Crystallization experiments were carried out with a racemic mixture of the inhibitor C11P. The conditions under which the ternary C11P−lipase−colipase complex was crystallized were very similar to those described in the case of the ternary phospholipid−lipase−procolipase complex (van Tilbeurgh et al., 1993a). At room temperature, C11P powder is soluble only in organic solvents. Two milligrams of this inhibitor was dissolved in 10 μL of THF (tetrahydrofuran). Two microliters of this solution was added to a solution containing 8 mg/mL lipase and 2.5 mg/mL colipase, which corresponds to a molar excess of inhibitor vs lipase of 100. After 30 min of incubation, 4 μL of this solution was mixed with 4 μL of the mother liquor containing 2% PEG 8000, 0.1 M MES (pH 6.0), and 0.4 M NaCl and deposited in the form of sitting drops. A few days later, 1 μL of an octyl β-glucoside solution in water (250 mM) was added to the drops, and tetragonal crystals developed overnight. They grew within about 2 days to a maximum size of 0.5 mm × 0.5 mm × 0.5 mm. Octyl β-glucoside actually induces the formation of crystals. Alternatively, octyl β-glucoside was added without any previous equilibration period; in this case, much more numerous but smaller crystals developed in each drop. These crystals belong to the space group $P4_22_12$ and are isomorphous ($a = b = 134.0$ Å and $c = 94.0$ Å) with those obtained in the case of the ternary phospholipid−lipase−colipase complex (van Tilbeurgh et al., 1992).

*Data Collection and Resolution of the Structure.* X-ray diffraction data were measured with a MAR-Research imaging plate detector with a diameter of 18 cm (Marresearch, Hamburg, Germany) mounted on a Rigaku RU200 rotating anode (running at 40 kV × 80 mA). The data were reduced using the image plate version of XDS (Kabsch, 1989a,b), and the statistics are given in Table 1. We used the 3.0 version of the X-PLOR program (Brünger, 1992) for crystallographic refinement and, for the last cycle of refinement, the 3.1 version, in which the Engh−Huber force field is used (Engh & Huber, 1991). The starting model was the lipase−colipase complex (without any bound ligand or water molecules), as determined in the ternary phospholipid−lipase−colipase structure (van Tilbeurgh et al., 1993). A standard simulated annealing protocol (SA) was used to refine the structure (Brünger, 1988). It consists of 300 cycles of conjugate gradient minimization followed by molecular dynamics (0.5 ps at 1500 K and 0.5 ps at 300 K), 400 steps of conjugate gradient minimization, and 15 cycles of restrained individual *B*-factor refinement. The initial round of refinement using reflections between 8.0 and 2.46 Å brought the *R*-factor down from 43.7% to 24.8%. $(2|F_o| - |F_c|)e^{i\alpha calc}$ and $(|F_o| - |F_c|)e^{i\alpha calc}$ difference maps were calculated between 20 and 2.46 Å resolution ($F_o$ and $F_c$ are observed and calculated structure factor amplitudes, respectively, and αcalc are calculated phases). The maps were inspected on Silicon Graphics workstations using the graphics TURBO program (Roussel & Cambillau, 1991). The water-accessible surface calculations were performed with the DSSP program (Kabsch & Sander, 1983).

## RESULTS

*Model Refinement.* After the initial rounds of the lipase−colipase complex refinement, residual ($2F_o - F_c$) and ($F_o - F_c$) electron densities could be clearly observed starting at the catalytic Ser152 Oγ atom, indicating the presence of a covalently bound molecule of the phosphonate inhibitor. The *R* enantiomer of the C11P inhibitor (CONF1) was fitted into the electron density map. Some small regions of lipase and colipase were reconstructed (e.g., residues 246−251 of lipase and residues 72−80 of colipase), and water molecules were introduced. After several cycles of simulated annealing refinement, a strong residual electron density was observed near Ser152. This density could account for the *S* enantiomer of the C11P inhibitor (CONF2) (Figure 1). We further refined partial occupancies for both enantiomers using the alternate conformation option of X-PLOR 3.0. The occupancies of the first and second conformations have been refined to 0.65 and 0.40, respectively, with *B*-values of 21.9 and 16.3 Å$^2$ (Table 1). These values are lower than the average *B*-factors for the complex as a whole. They are quite comparable, however, with the *B*-factor values obtained with residues from the active site (with 20 Å$^2$ in the case of Ser152 and 17 Å$^2$ in that of His263).

Five detergent molecules have been constructed in the residual density along the hydrophobic surface of the complex. The occupancy of these five octyl β-glucoside molecules was set at 0.5, and only their *B*-factors were refined. Two of these five molecules resisted further refinement (Figure 2). The third one lacked electron density at the glucose ring. The last two detergent molecules had a poorly defined electron density. We attempted to refine them using alternative conformations, keeping the glucose ring in a common position and giving the octyl chains two different orientations. The average *B*-factor of these two molecules was higher, however, than that of the first three (59.8 Å$^2$ on average versus 40.8 Å$^2$ ).

The final refinement statistics are given in Table 1. Besides the protein compounds, the model contains 1 covalent inhibitor (two enantiomers), 1 $Ca^{2+}$ ion, 293 water

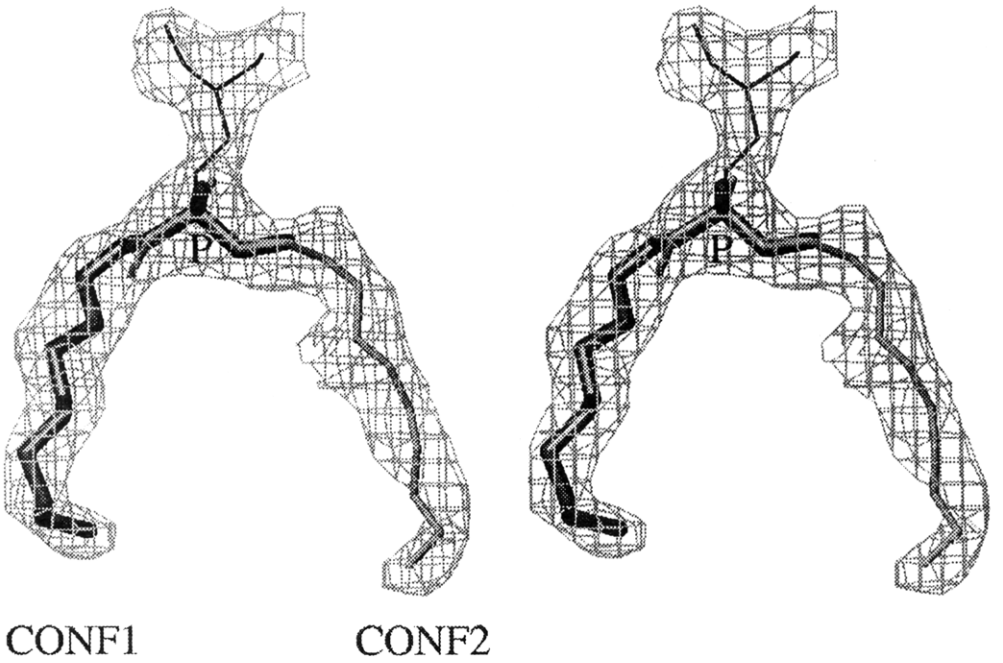


FIGURE 1: Stereographic view of the final residual electron density map of the C11P inhibitor, using coefficients ($2F_o - F_c$) and calculated phases ($F_o$ and $F_c$ are the observed and calculated structure factors). The active serine is covalently bound to either conformation of the inhibitor. In both enantiomers the position of the phosphorus atom of the inhibitor is similar: its distance from the catalytic serine O$\gamma$ is 1.62 Å in the first conformation (CONF1) and 1.65 Å in the second one (CONF2).

Table 1: Collection and Refinement Statistics

| | |
|---|---|
| data collection | |
| lowest resolution shell (Å) | 20.0−10.67 |
| highest resolution shell (Å) | 2.53−2.46 |
| total no. of obsd reflections (20−2.46 Å) | 271893 |
| no. of independent reflections (20−2.46 Å) | 29845 |
| completeness (%) (20−2.46 Å) | 92 |
| completeness (%) (2.53−2.46 Å) | 77.8 |
| $R_{sym}$ (%)[a] | 10.6 |
| % of $I > \sigma I$ (20−2.46 Å) | 94.6 |
| % of $I > \sigma I$ (2.53−2.46 Å) | 84.9 |
| redundancy (20−2.46 Å) | 9.4 |
| redundancy (2.53−2.46 Å) | 3.9 |
| refinement statistics | |
| no. of protein atoms | 5080 |
| no. of inhibitor atoms | 30 |
| no. of water molecules | 293 |
| no. of detergent atoms | 140 |
| resolution range (Å) | 6.0−2.46 |
| no. of reflections | 27738 |
| $R$-factor ($I/\sigma I > 1$)[b]/free $R$-factor[c] | 18.3/25.8 |
| rms deviation from ideal geometry of the final model | |
| bond distances (Å) | 0.013 |
| bond angles (deg) | 1.960 |
| av $B$-factor value (Å$^2$) | |
| main-chain atoms | 30.5 |
| side-chain atoms | 34.2 |
| inhibitor atoms (occupancy) | |
| conformation 1 | 21.9 (0.65) |
| conformation 2 | 16.3 (0.40) |
| solvent atoms | 44.7 |
| detergent atoms | |
| detergent molecules (occupancy) | 26.3 (0.5), 57.5 (0.5), 38.5 (0.5), 58.3 (0.5), 58.9 (0.5), 52.1 (0.5), 70.0 (0.5) |

[a] $R_{sym} = \sum_{hkl}\sum_{ref}|I_{hkl} - \langle I_{hkl}\rangle|/\sum_{hkl}\sum_{ref}\langle I_{hkl}\rangle$. [b] $R$-factor $= \sum_{hkl}|F_o - F_c|/\sum_{hkl}|F_o|$. [c] Brünger (1992).

molecules, and 5 detergent molecules (with partial occupancies, 2 have alternate conformations). Coordinates have been deposited with the Protein Data Bank.

*Conformational Changes of PL.* The most significant structural differences observed between the open and the closed form were conformational changes in the active site loops and a bending motion of the noncatalytic $\beta$-barrel domain (Figure 3). Structural transitions similar to those induced upon the binding of a phospholipid at the active site of pancreatic lipase (van Tilbeurgh et al., 1993b) were also observed in the present covalently inhibited complex. Moreover, the phospholipid ternary complex was found to be very similar to the covalently bound complex with regard to the rms deviation of 0.82 Å between the Cα coordinates of both structures. The most striking difference between the closed and open forms was that occurring at the surface loop

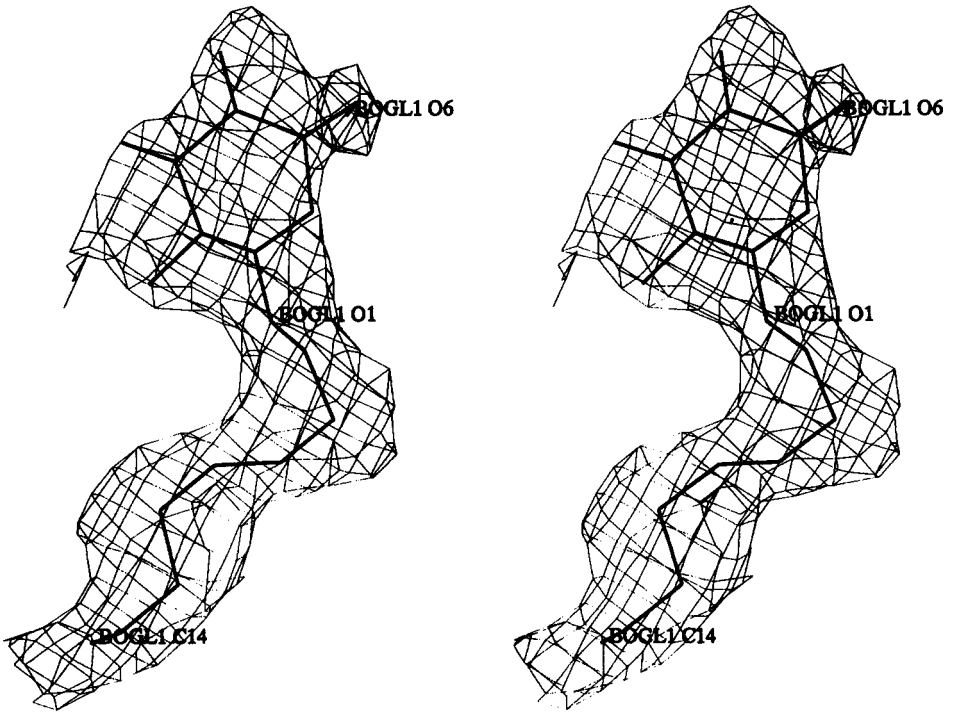


FIGURE 2: Stereographic view of the final residual electron density map of the octyl $\beta$-glucoside molecule BOGL1 [occupancy 0.5; coefficients are $(2F_o - F_c)$ with calculated phases].

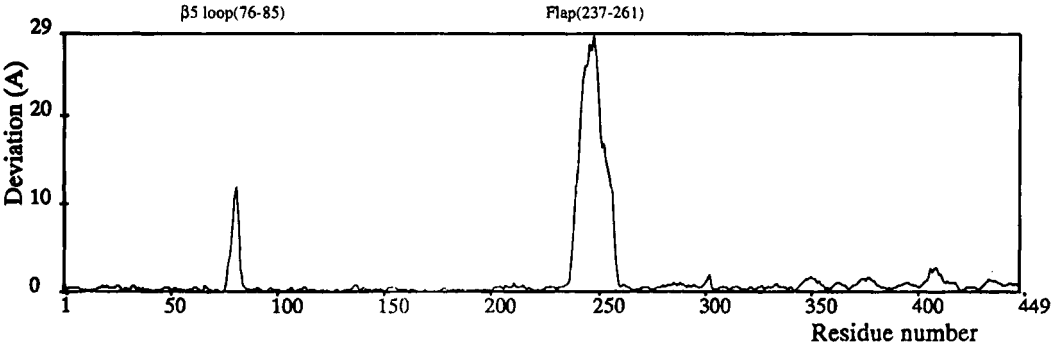


FIGURE 3: Plot of the difference between the positions of equivalent Cα atoms of the open and the closed form of the lipase, based on the structures of the ternary complex HPL/pCol/C11P and the native HPL (Winkler et al., 1990), respectively. The two peaks clearly indicate the drastic conformational changes in the $\beta$5 loop (residues 76−85) and the lid (residues 237−261). Small deviations at the end of the sequence account for the bending of the C-terminal domain.

formed by residues 237−261 (the lid), where each residue's conformational angles changed completely, and at the loop immediately following the fifth $\beta$-strand, comprising residues 76−85 (Table 2, Figure 4). The higher resolution of the present structure made it possible to give a more detailed comparison between the open and closed forms than in the case of the complex with phospholipid (van Tilbeurgh et al., 1993b).

The lid in the closed form makes few contacts with the remainder of the protein (Winkler et al., 1990). Only three direct hydrogen bonds were observed between the lid and the core of the protein. Seven hydrogen bonds within the lid further stabilize its closed conformation. The majority of these interactions were observed in the short distorted helix that blocks the active site between residues 247 and 254. The van der Waals contacts between the lid and the core of the catalytic domain are mainly due to Trp252, which fills the active site pocket and interacts with Phe77, Leu153, and Tyr114. A few water molecules, located between the lid and the surface of the catalytic crevice, may also contribute to stabilizing the closed conformation. The above-average *B*-factor values obtained with the residues of the lid in the closed form suggest that it is more labile than the rest of the structure.

In the open form, the lid is engaged in a much larger number of hydrogen bonds and salt bridges (Table 3). None of these interactions were found to exist in the closed conformation. First there are 14 internal H-bonds, which are mainly associated with the formation of the two amphipathic helices. These helices are tightly packed together, and a few hydrogen bonds exist between them. The first amphipathic helix makes three polar contacts with the colipase, while the hydrophilic side of the second amphipathic helix interacts with the catalytic crevice and the rest of the lipase body (three interactions, Table 3). The average *B*-factors of the main-chain atoms of the lid are much lower for its open form than for the closed one (37.7 and 49.8 Å$^2$, respectively). The total area of contacts made by the lid residues with the remainder of the complex is similar, however, in both conformations (1038 and 978 Å$^2$ in the closed form and in the open form, respectively).

The removal of Trp252 from the active site pocket induces an additional conformational change in the $\beta$5 active site surface loop. In the closed form, this loop abuts the lid,

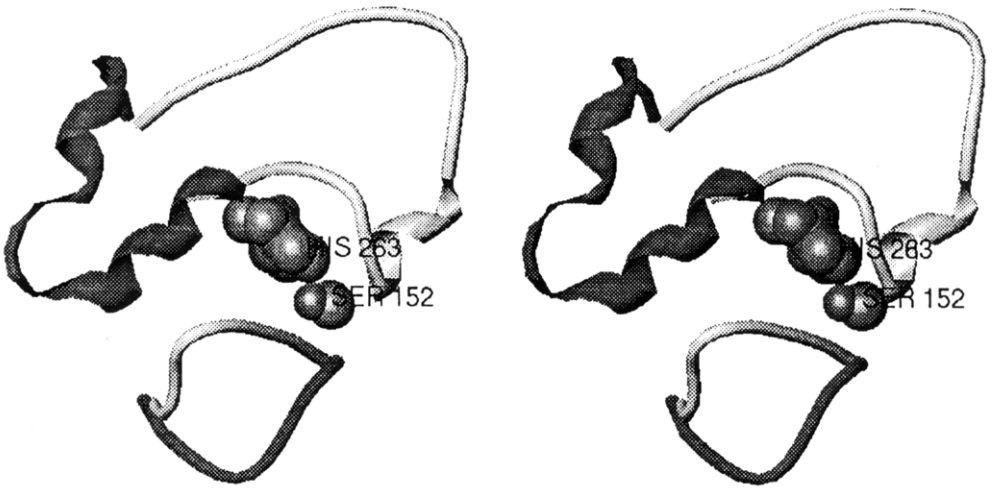


FIGURE 4: Stereographic view of the closed (light gray) and open (dark gray) conformations of the $\beta$5 loop (residues 76−85) and of the lid (residues 237−261). Residues of the catalytic triad are indicated.

Table 2: Conformational Angles (deg) of the Lid and the $\beta$5 Loop of the Open (C11P Complex) and Closed Conformation

| Lid | | | | | | |
|---|---|---|---|---|---|---|
| closed form | | | | open form | | |
| Φ | Ψ | secondary structure | residue | Φ | Ψ | secondary structure− |
| 85 | 144 | $\beta$ | K238 | −92 | 48 | $\beta$ |
| −84 | 140 | $\beta$ | K239 | −81 | 165 | $\beta$ |
| −81 | 154 | $\beta$ | N240 | −77 | 162 | $\beta$ |
| −70 | 130 | $\beta$ | I241 | −56 | −40 | α |
| −68 | 134 | $\beta$ | L242 | −74 | −29 | α |
| −138 | 138 | $\beta$ | S243 | −80 | −35 | α |
| −69 | −33 | α | Q244 | −63 | −51 | α |
| −120 | 135 | $\beta$ | I245 | −65 | −36 | α |
| −139 | 132 | $\beta$ | V246 | −100 | 62 | $\beta$ |
| −95 | 83 | $\beta$ | D247 | −102 | 164 | $\beta$ |
| −51 | −39 | α | I248 | −47 | −14 | α |
| −59 | −54 | α | D249 | −102 | 8 | |
| −60 | −44 | α | G250 | −106 | 164 | α |
| −54 | −52 | α | I251 | −67 | −45 | α |
| −59 | −34 | α | W252 | −59 | −41 | α |
| −83 | −8 | α | E253 | −66 | −41 | α |
| 79 | 18 | | G254 | −59 | −42 | α |
| −86 | −13 | α | T255 | −66 | −46 | α |
| −121 | 153 | $\beta$ | R256 | −53 | −45 | α |
| −67 | 136 | $\beta$ | D257 | −63 | −51 | α |
| −166 | 123 | $\beta$ | F258 | −61 | −41 | α |
| −87 | 108 | $\beta$ | V259 | −70 | −34 | α |
| −84 | −2 | | A260 | −167 | −50 | $\beta$ |
| $\beta$5 Loop | | | | | | |
| closed | | | | open | | |
| Φ | Ψ | secondary structure | residue | Φ | Ψ | secondary structure |
| −66 | 131 | | F77 | −45 | 142 | $\beta$ |
| −119 | 111 | $\beta$ | I78 | −59 | −20 | |
| −87 | 170 | $\beta$ | D79 | −79 | 178 | $\beta$ |
| −57 | 134 | $\beta$ | K80 | −138 | 161 | $\beta$ |
| 70 | 4 | | G81 | −73 | −12 | α |
| −98 | 2 | | E82 | −88 | 0 | |
| −52 | −19 | α | E83 | −52 | 142 | $\beta$ |
| −94 | 0 | α | D84 | −62 | −37 | $\beta$ |

and its conformation is maintained by hydrophobic interactions between Phe77 and Trp252. There exist only two hydrogen bonds between this loop and the rest of the catalytic domain. In the open form, the hydrophobic contact with the lid is interrupted, and this loop folds back upon the core. This conformation is stabilized by nine further hydrogen bonds: three with the lid and six with the remainder of the catalytic domain. The total area of contacts made by the residues of this loop with the remainder of the complex is 623 Å$^2$ in the closed form and 902 Å$^2$ in the open form.

Table 3: External Polar Interactions of the Lid

| lipase lid | lipase body | distance (Å) |
|---|---|---|
| Trp252 NE1 | Glu83 OE2 | 3.09 |
| Arg256 NH1 | Asp79 OD2 | 3.13 |
| Arg256 NH2 | Asp79 OD1 | 3.00 |
| Asp257 OD1 | Arg265 NH2 | 3.10 |
| lipase lid | colipase | distance (Å) |
| Asn240 N | Glu15 OE1 | 2.79 |
| Val246 O | Arg38 NH1 | 2.46 |
| Val246 O | Arg38 NH2 | 2.99 |

*Water-Accessible Surface.* Surprisingly, the water-accessible surface of lipase (not taking the colipase into account in the calculation) is somewhat smaller (by 450 Å$^2$) in the open form than in the closed form (Table 4E). The open lipase surface interacting with colipase amounts to 965 Å$^2$, which is divided into two contact areas, 660 Å$^2$ with the C-terminal domain and 305 Å$^2$ with the lid (Table 4E).

The hydrophobic water-accessible surface can be roughly subdivided into two main regions: the first one is the very hydrophobic groove lying next to the active serine, opposite the catalytic triad His263. This hydrophobic groove preexists in the closed form and becomes uncovered due to the rearrangement of the surface loops (Figure 5 and Table 4C). Adjacent to this groove is the hydrophobic surface of the $\beta$5 loop (Figure 5 and Table 4B). The second water-accessible hydrophobic surface is a hydrophobic plateau which is formed by the hydrophobic half-sides of the two amphipathic helices of the lid. The conformational change in the lid causes these hydrophobic residues to be clustered together. These surfaces are in contact with Phe77, which is probably stacked against the glycerol moiety of a bound substrate. The other members of the mammalian pancreatic lipase family have a large hydrophobic side chain at this position; e.g., lipoprotein lipase has a tryptophan at this position (van Tilbeurgh et al., 1993, 1994).

Important consequences of all the conformational changes were observed on the solvent-accessible hydrophobic surface of the lid and on that of the $\beta$5 loop and the groove (Figure 5, Table 4). Overall, the surface of the lid and that of the $\beta$5 loop decreased by 58 and 205 Å$^2$, respectively, from the closed to the open form, not including the colipase in the calculation (Table 4A,B). The interaction of the lid with

Table 4: Sum of the Water-Accessible Surfaces (in Å$^2$) of Residues of the Lid (A), the β5 Loop (B), and the Active Site Groove (C) Calculated in the Closed Lipase and Open Lipase, in the Absence (Lip/Closed and Lip/Open) or Presence of Colipase (Lipcol/Open),[a] (D) Sum of the Water-Accessible Surfaces (in Å$^2$) by Residue Class, and (E) Overall Water-Accessible Surfaces (in Å$^2$) in the Closed Lipase and Open Lipase

(A) Lid

| residue class | (1) lipase, closed form | (2) lipase, open form | (2) − (1) | (4) lipase−colipase, open form | (4) − (2) |
|---|---|---|---|---|---|
| C | 841 | 465 | −376 | 405 | −60 |
| S | 374 | 278 | −96 | 141 | −137 |
| H | 506 | 920 | 414 | 812 | −108 |
| total | 1721 | 1663 | −58 | 1358 | −305 |

(B) β5 Loop

| residue class | (1) lipase, closed form | (2) lipase, open form | (2) − (1) |
|---|---|---|---|
| C | 366 | 113 | −253 |
| S | 176 | 118 | −58 |
| H | 54 | 160 | +106 |
| total | 596 | 391 | −205 |

(C) Active Site Groove

| residue class | (1) lipase, closed form | (2) lipase, open form | (2) − (1) |
|---|---|---|---|
| S | 110 | 223 | +113 |
| H | 124 | 520 | +396 |
| total | 234 | 743 | +509 |

(D) Sum of the Water-Accessible Surfaces by Residue Class

| residue class | lid | β5 loop | active site groove | total |
|---|---|---|---|---|
| C | −376 | −253 | | −629 |
| S | −96 | −58 | +113 | −41 |
| H | +414 | +106 | +396 | +916 |

(E) Overall Water-Accessible Surfaces

| (1) lipase, closed form | (2) lipase, open form | (3) lipase−colipase, open form | (4) colipase | (2) − (1) | (4) − [(3) − (2)]/2[b] | colipase/lid | colipase/(C-terminal domain of lipase) |
|---|---|---|---|---|---|---|---|
| 18517 | 18060 | 21752 | 5622 | −450 | 965 | 305 | 660 |

[a] Residue classes (charged, semipolar, and hydrophobic) are indicated by the letters C (charged: Arg, Asp, Glu, His, Lys), S (semipolar: Gln, Asn, Cys, Gly, Ser, Thr), and H (hydrophobic: Ala, Ile, Leu, Phe, Pro, Trp, Tyr, Val), respectively. [b] Result is colipase surface in interaction with lipase.

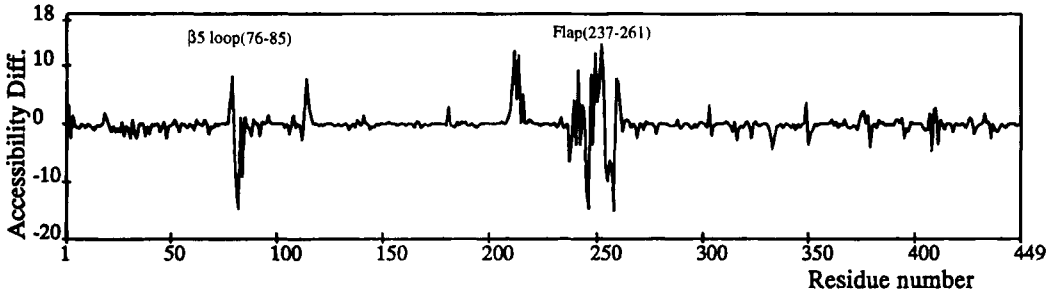


FIGURE 5: Plot of the differences between the water-accessible surfaces of open and closed lipase (sign: open − closed). The surfaces have been normalized in terms of the number of atoms per residue.

colipase masked another 305 Å$^2$ of the lid surface. Upon roughly distributing the amino acids into three classes (charged, C; semipolar, S; hydrophobic, H; Table 4), however, we noted a large increase in the hydrophobic accessible surface of the lid and of the β5 loop along with a decrease in the charged accessible surface (Table 4A,B); whereas in the case of the active site groove, both the semipolar and the hydrophobic surface increased, and this was entirely due to the removal of the lid. All in all, a considerable increase in the exposed hydrophobic surface (+916 Å$^2$) and a comparable decrease in the exposed charged surface (−629 Å$^2$) occurred, whereas the exposed semipolar surface remained almost constant (Table 4D).

*Structure of the Bound Inhibitor.* The alkyl portions of the two C11P enantiomers superimpose well with the two fatty acid acyl chains of the phospholipid (Figure 6) observed in the ternary phospholipid complex (van Tilbeurgh et al., 1993b). The fact that the oxygen of the phosphorus ester (O1) in both enantiomer structures forms a hydrogen bond with the main-chain nitrogens of Leu153 and Phe77 confirms the earlier hypothesis about the role of these residues in oxyanion stabilization. The geometry of this oxyanion hole is very similar to that observed in the other two adducts with RML or cutinase (Figure 7) (Brzozowski et al., 1991; Martinez et al., 1994). The methoxy oxygen of the first enantiomer (CONF1) forms a hydrogen bond with the Nε of His263 (Figure 8a). In the second enantiomer structure (CONF2), the methoxy oxygen does not form any hydrogen bond (Figure 8b).

The C11P inhibitor is much more effective at inhibiting pancreatic lipase than the short-chain organophosphate compounds are (Cudrey et al., 1993; Marguet et al., 1994). The efficiency of this inhibitor can be assessed from the interactions between the long hydrophobic C11-alkyl chain and the residues of the active site (Figure 9). The C11-alkyl chain of the first conformation (highest occupancy) lies in

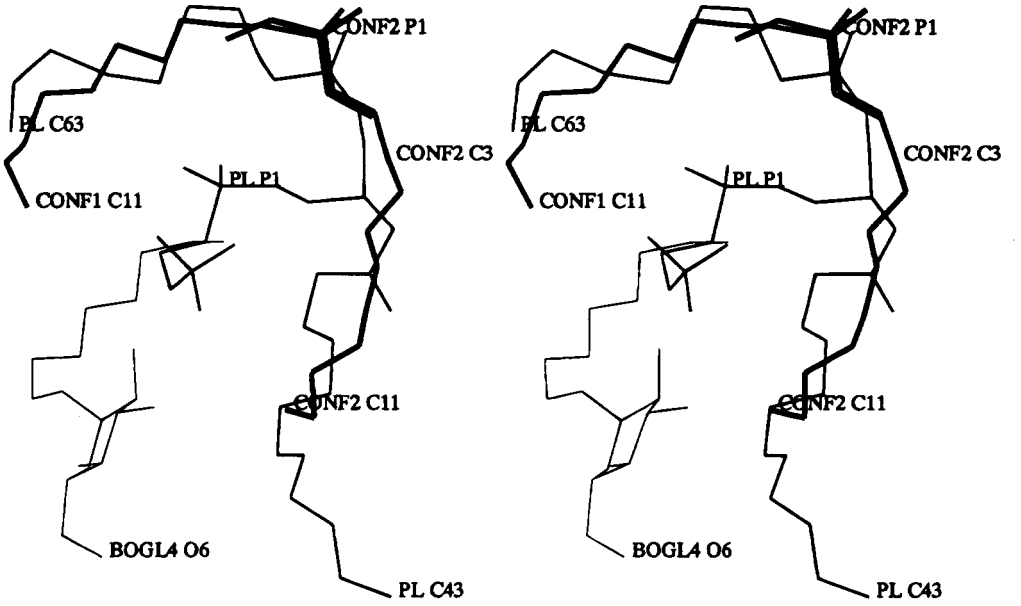


FIGURE 6: Stereographic view of the phosphatidylcholine molecule [as refined in the ternary lipase−colipase−mixed micelle complex (van Tilbeurgh et al., 1993b)] superimposed on the two enantiomers of the C11P inhibitor and on the nearest octyl $\beta$-glucoside molecules.

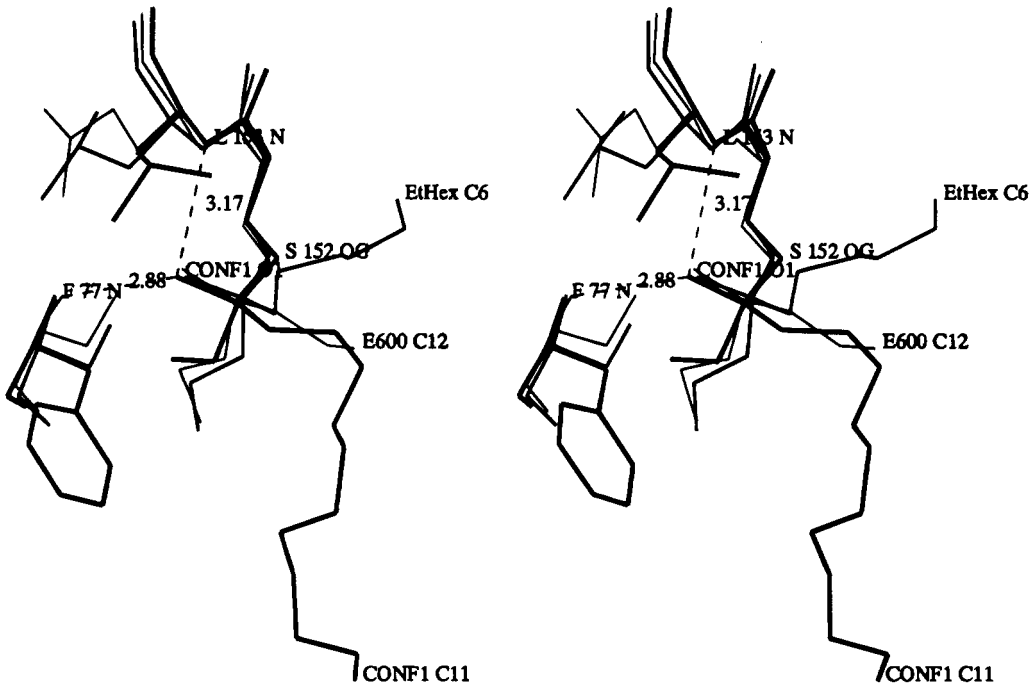


FIGURE 7: Stereographic view of the superimposition of the oxyanion hole and the organophosphate inhibitors as observed in the structures of cutinase−E600 (Martinez et al., 1994), *R. miehei*−EtHex C6 (Brzozowski et al., 1991), and human pancreatic lipase−C11P (lines from thin to thick). Superimposition is based on the oxyanion hole atoms, the O$\gamma$ of the catalytic serines, and the phosphorus oxygen.

the hydrophobic groove opposite His263. This groove starts at Ser152 and runs toward the surface of the enzyme. The C11 chain makes van der Waals contacts with the hydrophobic side chains forming the floor of this groove (Ala178, Phe215, Pro180, Tyr114, Leu213) (Figure 9). The alkyl chain has an elongated binding mode, and most of the bonds have a trans conformation. The alkyl chain reaches the surface but does not fill the whole groove. The ultimate methylene groups of the C11 chain protude from the enzyme's active site, leaving the hydrophobic groove at the end. Instead of making interactions with the enzyme they rather seem to be stacked with other hydrophobic molecules bound at the active site entrance. The complete groove might possibly accommodate about 14 methylene groups.

No side-chain rearrangements were observed for the residues in this groove when compared to those in the closed, unliganded form of the enzyme. The only noteworthy exception is Phe215, whose $\chi 1$ angle rotated through 110°, as observed also in the ternary HPL/pCol/phospholipid complex. This phenylalanine makes extensive hydrophobic contacts with the inhibitor (Figure 9). The methoxy group of the first enantiomer of C11P is located in front of a very hydrophilic pocket next to Ser152. This pocket contains a cluster of charged residues: Asp79 forming a salt bridge with Arg256, His263, His151, and a few well-defined water molecules. The methoxy oxygen of this enantiomer forms a hydrogen bond with the NE2 atom of His263 (Figure 8a) and is also very close to the O$\gamma$ of Ser152.

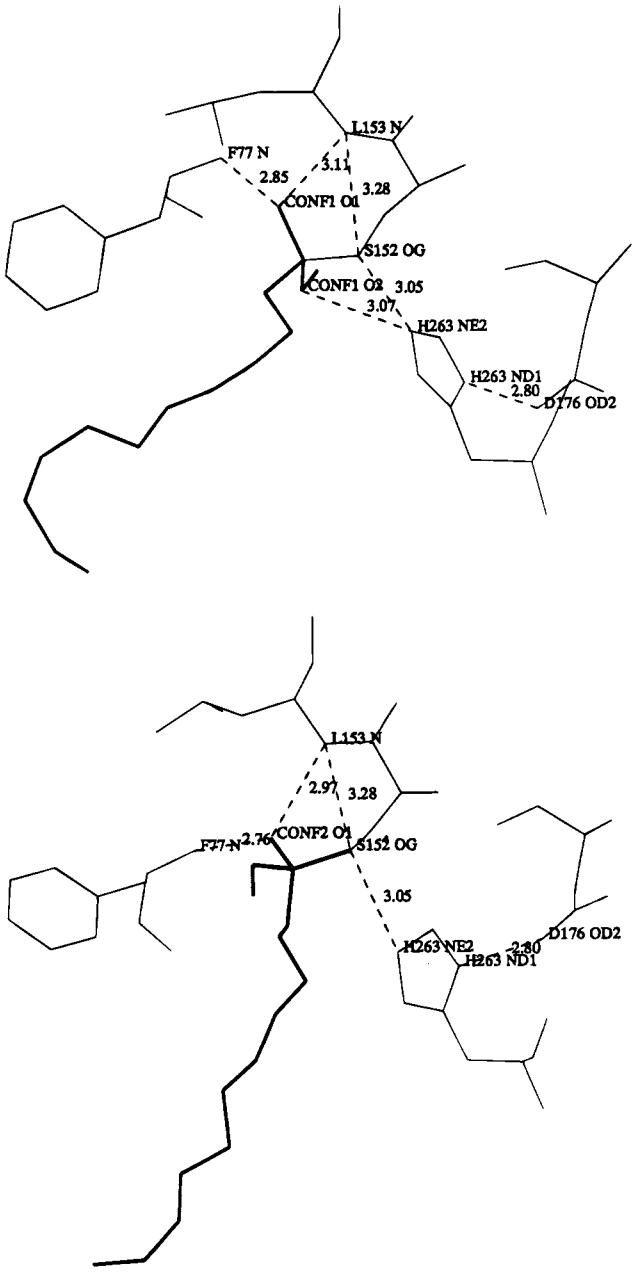


FIGURE 8: Polar interactions between the active site residues and (a) the first enaniomer of C11P (CONF1) and (b) the second enantiomer of C11P (CONF2).

The phosphorus atom of the second enantiomer occupies about the same position as in the case of the first enantiomer (Figures 1 and 6). The alkyl chain of the second enantiomer follows a hydrophobic patch on the surface of the open lid toward the rim of the active site (Figure 9). The methylene carbons which are closest to the P atom overlap with the methoxy group of the first enantiomer structure (Figure 6). The alkyl chain further runs parallel to the Arg256 side chain and reaches the surface near Trp252. This chain is also close to the hydrophobic tail of bound detergent molecules at the entrance to the active site (see below).

*Detergent Molecules and Crystal Packing.* Octyl $\beta$-glucoside, at a concentration above its critical micellar concentration, induces the crystallization of ternary lipase–colipase complexes (van Tilbeurgh et al., 1993a). Some residual electron density was still present after extensive refinement at the molecular surface of the complex. We modeled five octyl $\beta$-glucoside molecules into these electron densities but only partly succeded in refining these molecules (Table 1).

The octyl $\beta$-glucoside molecules are situated on the same face of the complex, that of the lipase lid and of the colipase finger tips (Figure 10). They are stabilized by interactions with the inhibitor, with hydrophobic residues from the open lid and the $\beta$5 loop, and with other hydrophobic residues belonging to the surface of lipase or colipase. Moreover, in view of the crystal packing, they are stacked between the hydrophobic faces of four symmetry-related complexes (Figure 11) (see below).

The best defined octyl $\beta$-glucoside molecule (BOGL1) is situated at the entrance to the active site, where it is sandwiched in a crystallographic contact. The glucose ring is stacked against the indole ring of Trp252, a situation which is frequently observed in protein–sugar interactions (Figure 12a). The OH groups form hydrogen bonds with residues from the $\beta$5 loop. The octyl chain is nearly parallel to the hydrophobic side of the second amphipathic helix of the lid and also forms interactions with hydrophobic residues of a symmetry-related molecule in the crystal, which may possibly explain why this compound is necessary to obtain crystals (the closed form of the pancreatic lipase complex does not, however, display this particular interaction with octyl $\beta$-glucoside but also needs the detergent to be crystallized). Another detergent molecule (BOGL3) is hidden in a cavity formed by the N-terminal domain of lipase and colipase (Figure 12b). The hydroxyl groups are hydrogen bonded to residues from lipase and from colipase, either directly or via bound water molecules. The octyl chain lies against a hydrophobic patch on one side of the second finger of colipase (carbons of Arg38, Leu36, etc.). In the case of the third interesting octyl $\beta$-glucoside molecule, the glucosyl moiety did not resist the refinement: the $(2|F_o| - |F_c|)$ map provides evidence for the existence of only an alkyl chain, wedged between the two conformations of the C11 inhibitor alkyl chains at the active site. This density might also correspond to an unreacted phosphonate inhibitor, from which its C11-alkyl chain projects into the active site and its hydrophilic head group into the solution.

The crystallographic packing requires some comments. The packing in the crystals can best be described as a dimer of dimers (Figure 11). Here two lipase–colipase complex molecules form a side to side dimer. The extensive hydrophobic surface of this dimer, formed jointly by the active site region of lipase and by the hydrophobic extremities of the colipase fingers, lies opposite the equivalent hydrophobic surface of the dimer packing partner in the crystal. These hydrophobic surfaces do not interact directly. Elongated residual electron density stretches, caught between these surfaces, were observed after the final round of refinement. It is difficult to interpret these densities, but in view of the highly hydrophobic environment, we propose that they are probably reporting detergent and/or inhibitor molecules. One example of a detergent molecule mediating crystal contacts has already been described above. A second case is shown in Figure 12b (BOGL3). A weakly bound detergent molecule bridges the hydrophobic fingers of symmetry-related colipase molecules in the crystal (Figure 12c).

## DISCUSSION

The active sites of those triglyceride lipases having known three-dimensional structures are covered by one or more surface loops (Winkler et al., 1990; van Tilbeurgh et al.,

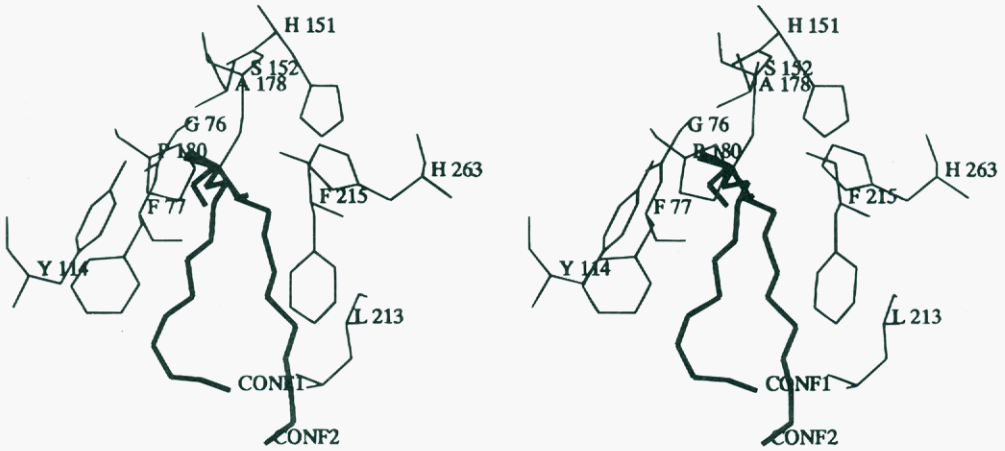


FIGURE 9: Stereographic picture of the interactions of both enantiomers of the inhibitor C11P with the active site serine and the residues of the hydrophobic groove of the lipase.

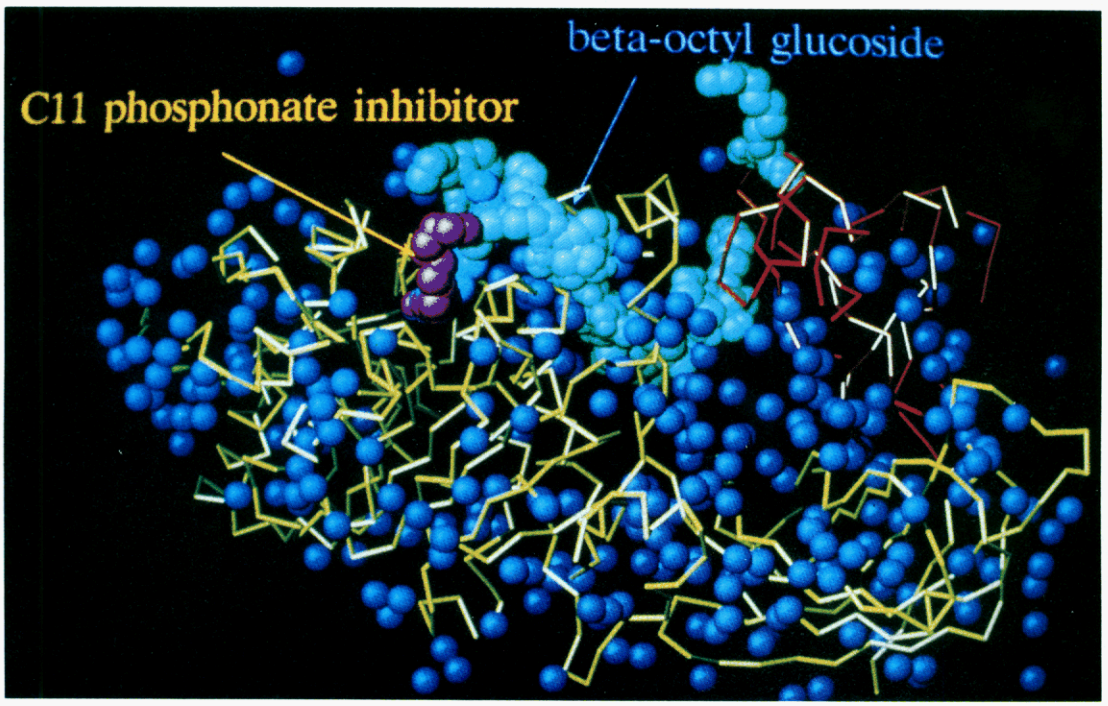


FIGURE 10: Color picture of the ternary complex HPL/pCol/C11P: HPL in yellow, colipase in red, C11P molecules in pink, octyl $\beta$-glucoside molecules in green, and water molecules in blue.

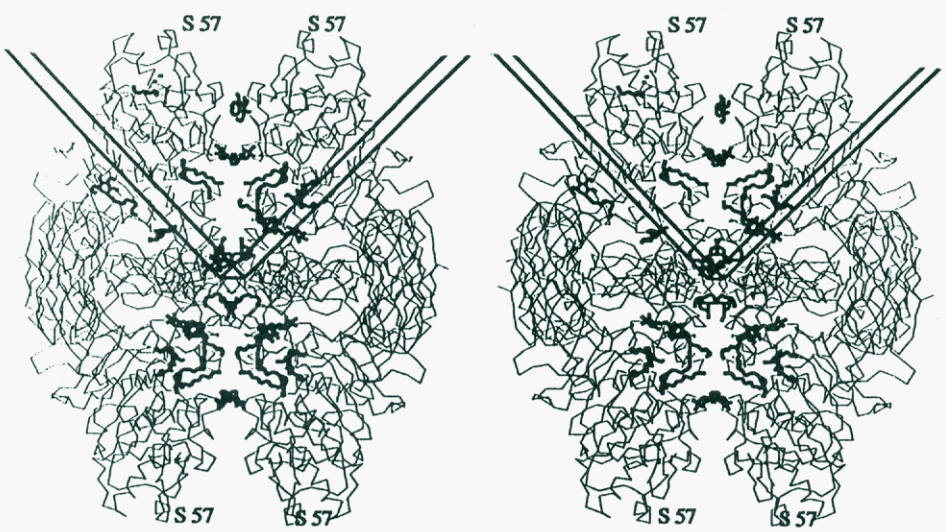


FIGURE 11: Stereographic view of the "crystallographic tetramer" formed by four symmetry-related molecules of the ternary complex. Octyl $\beta$-glucoside and inhibitor molecules (in thick lines) are mainly situated at the hydrophobic interface situated between the complexes and as a result of this crystal packing.

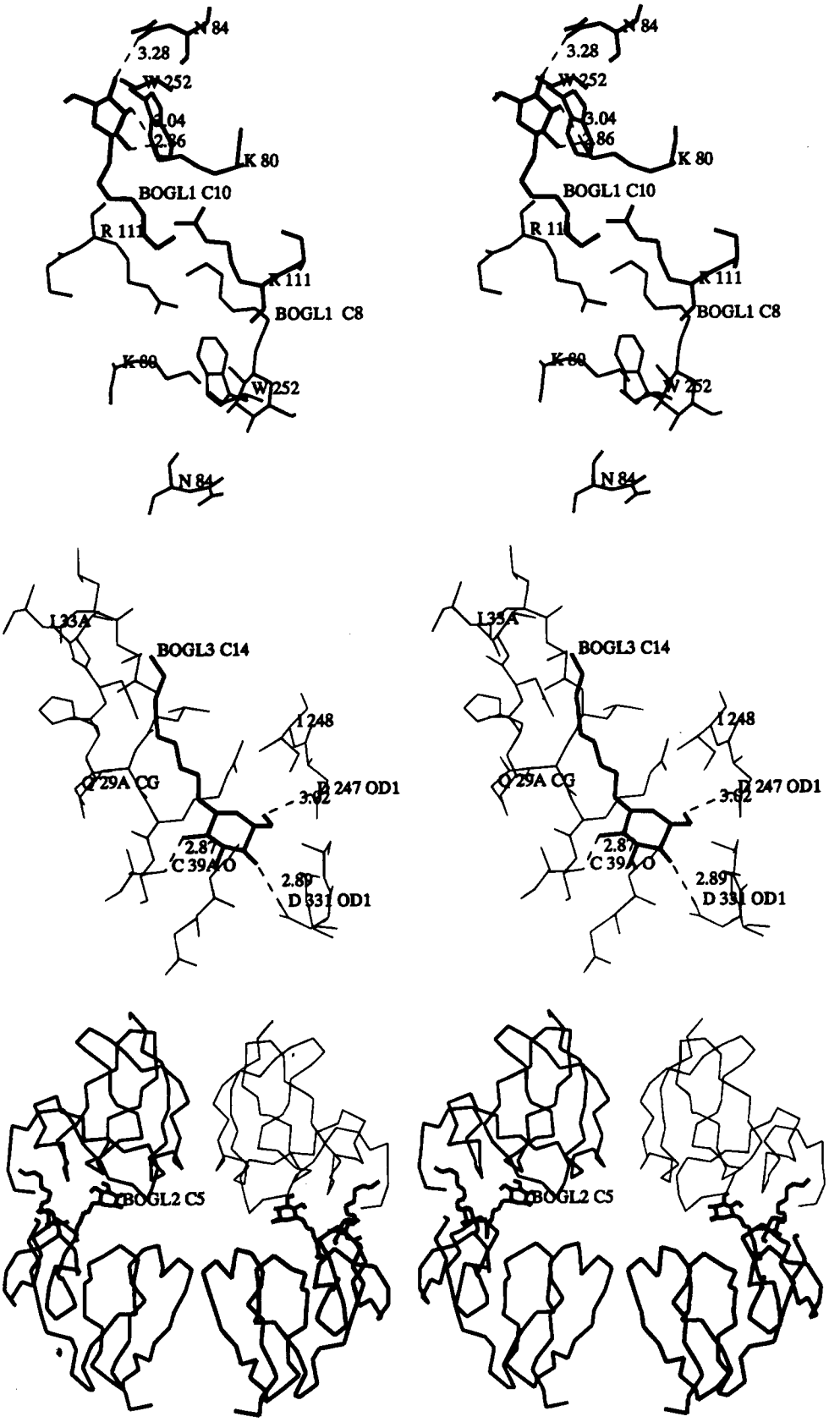


FIGURE 12: Stereographic view (a) of octyl $\beta$-glucoside BOGL1 stacked against W252 and the symmetry-related part, (b) of octyl $\beta$-glucoside BOGL3 in a cavity between the N-terminal domain of lipase and colipase, and (c) of octyl $\beta$-glucoside BOGL2 sandwiched between symmetry-related colipase molecules.

1992; Brady et al., 1990; Schrag et al., 1991; Noble et al., 1993). It is believed that this closed form is the preferred state in solution. Upon covalent modification of the active site serine, these surface loops are removed from the active site pockets, and the resulting open conformation probably constitutes the catalytically active state of the enzyme. In the case of three of them, the opening of the active site has been described from the structural point of view. In the lipase from *R. miehei*, the conformational changes essentially involve rigid body movements of the blocking helix (Brady

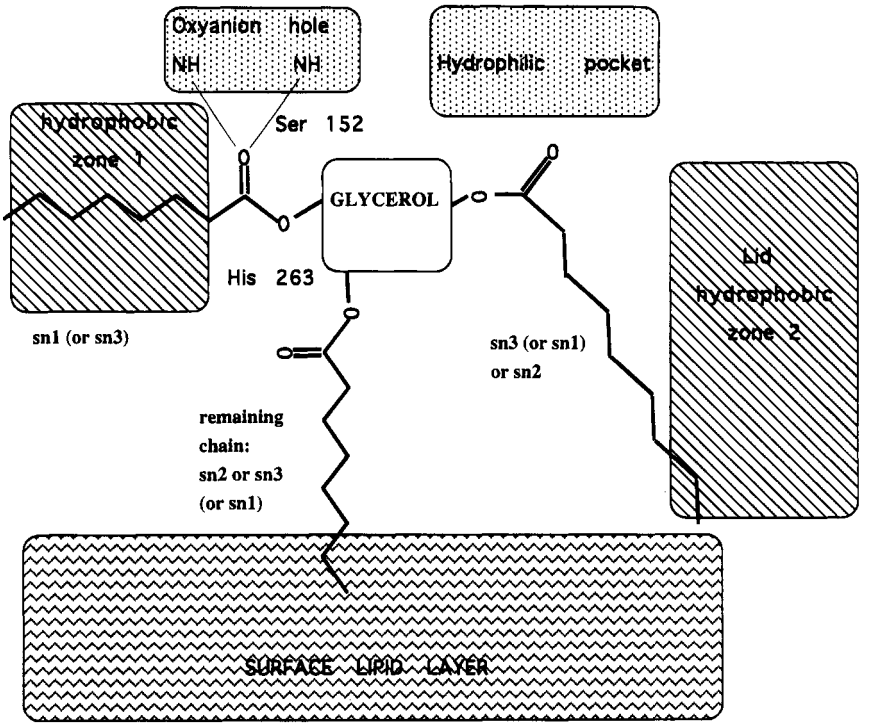


FIGURE 13: Diagram of the binding mode of a triglyceride (trioctanoyl) in the active site crevice of pancreatic lipase.

et al., 1991; Derewenda et al., 1992). In the case of the *C. rugosa* lipase, the opening of the lid includes a *cis* to *trans* isomerization of a proline residue together with some additional changes in the conformational angles (Grochulski et al., 1993, 1994a,b). The most complex transition observed to date is that in the pancreatic lipase lid, where the conformational angles of almost every residue are changed. In the open conformation of this enzyme, the lid is stabilized by a considerably larger number of hydrogen bonds than it is in the closed form. The residues involved in interactions between the lid and the core and between the lid and colipase are all strictly conserved among the pancreatic lipase sequences (Carrière et al., 1994). Interestingly, many of these core residues have been substituted in the sequence of the guinea pig pancreatic (phospho)lipase, which is 78% homologous with that of human lipase but has a truncated lid of only five residues (Hjorth et al., 1993). This lipase is inhibited by bile salts when its activity is tested on long-chain triacylglycerols but is not reactivated by colipase (Thirstrup et al., 1994).

Although the structure of the open pancreatic lipase lid has by now been well documented, neither the opening mechanism nor the functional role of the lid has been yet completely elucidated. One possibility is that there may exist a dynamic equilibrium between the open and the closed forms, the latter being the predominant conformation in solution (pancreatic lipase still has some residual activity on water-soluble substrates). The hydrophobic interface might shift this equilibrium toward the open conformation of the enzyme by coating the hydrophobic surface created. Another possibility is that the interface may trigger the opening of the lid, in the absence of preequilibrium. In that case, the interface may "melt" the closed conformation of the lid (which is poorly stabilized) and induce the formation of the amphipathic helices, finally yielding a more stable structure. Many peptidic hormones tend to acquire an amphiphilic secondary structure when exposed to amphiphilic environments such as lipid water interfaces (Kaiser & Kézdy, 1987). The lack of knowledge about the molecular arrangement of surface lipids makes it difficult to speculate about the possible interaction between pancreatic lipase and triglyceride particles. Surface tension measurements of pancreatic lipase at lipid monolayers have shown that the penetrating power of this enzyme is not significantly higher than that of standard globular proteins. Various proteins in fact inhibit the hydrolysis of triacylglycerol by lipases because they are irreversibly adsorbed at the lipid−water interface (Piéroni et al., 1990). It is a well-known fact that the lipid−water interface is a very denaturing environment for many proteins (even for lipases) (Rietsch et al., 1977). Given the complexity of the conformational transitions and the very high turnover numbers of pancreatic lipase, once bound the lipase−colipase complex probably never leaves the lipid particle before digestion has been completed (Rietsch et al., 1977).

The exact role of the lid in the lipolytic process is still rather elusive. The lid seems to be responsible for the interfacial activation phenomenon, which can also be said to inhibit the hydrolysis of substrates in the soluble form. Two highly active lipolytic enzymes, one of which does not have a lid (cutinase) and one whose lid is severely truncated [guinea-pig (phospho)lipase], lack the interfacial activation phenomenon but are nevertheless efficient triglyceride lipases (Martinez et al., 1992; Hjorth et al., 1993). The interaction between lipase and a lipid particle may not only change the lipase structure, as shown clearly by X-ray crystallography, but may also perturb the arrangement of lipid molecules in the surface layer of the contact zone. The hydrophobic surface around the active site may help to extract lipid molecules from the interface and to inject them into the active site. The lid may confer a functional advantage on pancreatic lipase under physiological conditions, where the enzyme is in competition with a whole panoply of dietary biomolecules for binding the lipid−water interface.

The opening of the lid in pancreatic lipase uncovers two hydrophobic zones, starting close to Ser152. The alkyl chain

of the enantiomer refined with the highest occupancy (CONF1, absolute configuration *R*) lies in the first zone (hydrophobic zone 1), running toward the surface of the enzyme. On the basis of the pancreatic lipase stereo preference, we can assume that this is the binding site for either the *sn-1* or the *sn-3* acyl chain of the substrate. This binding mode would place the carbonyl bond of the acyl-enzyme intermediate in an excellent position to be broken down by a water molecule. The acyl chain would be directed away from His263, which is well positioned to assist this reaction step (Figure 8a). Preliminary handmade modeling shows that introducing the *sn-2* acyl chain in this binding site may result in steric clashes. The alkyl chain of the second inhibitor enantiomer follows a hydrophobic path on the lid (hydrophobic zone 2). This may correspond to the binding of another acyl chain of a triglyceride substrate. Further studies are required to determine whether this acyl chain is *sn-1* or *sn-3* (corresponding to the binding of *sn-3* or *sn-1* into the first hydrophobic zone, respectively) or even *sn-2* (Figure 13). There is apparently no well-defined binding site for the third acyl chain, which again may be *sn-1*, *sn-3*, or *sn-2* (Figure 13). This third chain probably remains anchored in the lipid layer, which would make for rapid removal of the reaction products. The two hydrophobic zones at the active site are separated by a hydrophilic pocket which may interact with the polar atoms of the substrate's glycerol backbone and which may harbor the hydrolytic water molecules.

The positions of the alkyl chains of the two enantiomers of the C11 inhibitor are almost superimposable on the acyl chains of the previously described phospholipid (Figure 6). On the basis of these findings, we propose a scenario for the binding of triglyceride substrates at the active site (Figure 13). After partly leaving the lipid particle, the scissile acyl chain (*sn-1* or *sn-3*) of the substrate may bind to the hydrophobic groove, implying that the substrate adopts a "fork" conformation at the active site.

After the formation of the acyl-lipase intermediate and removal of the diglyceride, the active serine−fatty acid ester bond would be suitably positioned for being hydrolyzed by a water molecule, probably base-assisted by His263. It seems logical that this fatty acid should occupy the well-defined hydrophobic groove since it will remain into the active site until the breakdown of the acyl intermediate has occurred. To have it well oriented, out of the way of His263, may be a requirement for the efficient hydrolysis of the covalent intermediate.

## REFERENCES


Brady, L., Brzozowski, A. M., Derewenda, Z. S., Dodson, E., Dodson, G., Tolley, S., Turkenburg, J. P., Christiansen, L., Huge-Jensen, B., Norskov, L., Thim, L., & Menge, U. (1990) *Nature 343*, 767−770.

Brünger, A. T. (1988) *J. Mol. Biol., 203*, 803−816.

Brünger, A. T. (1992) *X-PLOR Version 3.1 Manual*, Yale University Press, New Haven, CT.

Brzozowski, A. M., Derewenda, U., Derewenda, Z. S., Dodson, G. G., Lawson, D. M., Turkenburg, J. P., Bjorkling, F., Huge-Jensen, B., Patkar, S. A., & Thim, L. (1991) *Nature 351*, 491−494.

Canioni, P., Julien, R., Rathelot, J., Rochat, H., & Sarda, L. (1979) *Biochimie 59*, 919−925.

Carrière, F., Thirstup, K., Boel, E., Verger, R., & Thim, L. (1994) *Protein Eng.* (in press).

Cudrey, C., van Tilbeurgh, H., Gargouri, Y., & Verger, R. (1993) *Biochemistry 32*, 13800−13808.

Cygler, M., Grochulski, P., Kazlauskas, R. J., Schrag, J. D., Bouthilier, F., Rubin, B., Serreqi, A. N., & Gupta, A. K. (1994) *J. Am. Chem. Soc. 116*, 3180−3186.

DeCaro, H., Figarella, C., Amic, J., Michel, R., & Guy, O. (1977) *Biochim. Biophys. Acta 490*, 411−419.

Derewenda, Z. S., & Derewenda, U. (1991) *Biochem. Cell Biol. 69*, 842−851.

Derewenda, U., Brzozowski, A., Lawson, D., & Derewenda, Z. (1992) *Biochemistry 31*, 1532−1541.

Engh, R. A., & Huber, R. (1991) *Acta Crystallogr. A47*, 392−400.

Grochulski, P., Li, Y., Schrag, J. D., Bouthilier, F., Smith, P., Harrison, D., Rubin, B., & Cygler, M. (1993) *J. Biol. Chem. 268*, 12843−12849.

Grochulski, P., Bouthilier, F., Kazlauskas, R. J., Serreqi, A. N., Schrag, J. D., Ziomek, E., & Cygler, M. (1994a) *Biochemistry 33*, 3494−3500.

Grochulski, P., Li, Y., Schrag, J., & Cygler, M. (1994b) *Protein Sci. 3*, 82−91.

Hjörth, A., Carrière, F., Cudrey, C., Wöldike, H., Boel, E., Lawson, D. M., Ferrato, F., Cambillau, C., Dodson, G. G., Thim, L., & Verger, R. (1993) *Biochemistry 32*, 4702−4707.

Kabsch, W. (1988a) *J. Appl. Crystallogr. 21*, 67−71.

Kabsch, W. (1988b) *J. Appl. Crystallogr. 21*, 916−924.

Kabsch, W., & Sander, C. (1983) *Biopolymers 22*, 2577−2637.

Kaiser, E. T., & Kézdy, F. J. (1987) *Annu. Rev. Biophys. Biophys. Chem. 16*, 561−581.

Kirchgessner, T. D., Chuat, J.-C., Heinzmann, C., Etienne, J., Guilhot, S., Svenson, K., Ameis, D., Pilon, C., D'Auriol, L., Andalibi, A., Schotz, M., Galibert, F., & Lusis, A. J. (1989) *Proc. Natl. Acad. Sci. U.S.A. 86*, 9647−9651.

Kraut, J. (1977) *Annu. Rev. Biochem. 46*, 331−358.

Marguet, F., Cudrey, C., Verger, R., & Buonu, G. (1994) *Biochim. Biophys. Acta 1210*, 157−166.

Martinez, C., De Geus, P., Lauwereys, M., Matthysens, G., & Cambillau, C. (1992) *Nature 356*, 615−618.

Martinez, C., Nicolas, A., van Tilbeurgh, H., Egloff, M.-P., Cudrey, C., Verger, R., & Cambillau, C. (1994) *Biochemistry 33*, 83−89.

Noble, M., Cleasby, A., Johnson, L., Egmond, M., & Frenken, L. (1993) *FEBS Lett. 331*, 123−128.

Ollis, D. L., Cheah, E., Cygler, M., Dijkstra, B., Frolow, F., Franken, S. M., Harel, M., Remington, S. J., Silman, I., Schrag, J., Sussman, J., Verschueren, K., & Goldman, A. (1992) *Protein Eng. 5*, 197−211.

Piéroni, G., Gargouri, Y., Sarda, L., & Verger, R. (1990) *Adv. Colloid Interface Sci. 32*, 341−378.

Rietsch, J., Pattus, F., Desnuelle, P., & Verger, R. (1977) *J. Biol. Chem. 252*, 4313−4320.

Roussel, A., & Cambillau, C. (1991) in *Silicon Graphics Directory*, Silicon Graphics, Mountain View, CA.

Schrag, J., Li, Y., Wu, S., & Cygler, M. (1991) *Nature 351*, 761−764.

Schrag, J., Winkler, F., & Cygler, M. (1992) *J. Biol. Chem. 267*, 4300−4303.

Thirstrup, K., Verger, R., & Carrière, F. (1994) *Biochemistry 33*, 2748−2756.

van Tilbeurgh, H., Sarda, L., Verger, R., & Cambillau, C. (1992) *Nature 359*, 159−162.

van Tilbeurgh, H., Gargouri, Y., Dezan, C., Egloff, M. P., Nésa, M.-P., Rugani, N., Sarda, L., Verger, R., & Cambillau, C. (1993a) *J. Mol. Biol. 229*, 552−554.

van Tilbeurgh, H., Egloff, M.-P., Martinez, C., Rugani, N., Verger, R., & Cambillau, C. (1993b) *Nature 362*, 814−820.

van Tilbeurgh, H., Roussel, A., Lalouel, J.-M., & Cambillau, C. (1994) *J. Biol. Chem. 269*, 4626−4633.

Verger, R. (1984) *Lipases* (Borgström, B., & Brockman, H. L., Eds.) Elsevier, Amsterdam.

Winkler, F. K., D'Arcy, A., & Hunziker, W. (1990) *Nature 343*, 771−774.


BI941689L